ACS EARTH AND SPACE CHEMISTRY

http://pubs.acs.org/journal/aesccq

Article

Effect of Ammonium Salts on the Decarboxylation of Oxaloacetic Acid in Atmospheric Particles

Alexandra L. Klodt, Kimberly Zhang, Michael W. Olsen, Jorge L. Fernandez, Filipp Furche, and Sergey A. Nizkorodov*

Cite This: *ACS Earth Space Chem.* 2021, 5, 931−940

Read Online

ACCESS | Metrics & More | Article Recommendations | Supporting Information

ABSTRACT: Oxaloacetic acid (OAA) is a 3-oxocarboxylic acid formed from the oxidation of succinic acid. OAA and other 3-oxocarboxylic acids experience a decarboxylation reaction in aqueous solutions, which can be catalyzed by ammonium and amines. This catalysis has not been studied under atmospherically relevant conditions despite previous interest in OAA in the atmosphere. To address this, 1 mM solutions of OAA were prepared with varying concentrations of ammonium sulfate, ammonium bisulfate, ammonium chloride, and sodium sulfate to simulate various atmospheric conditions. The extent of the decarboxylation was monitored using UV−visible absorption spectroscopy. OAA's uncatalyzed decarboxylation lifetime was around 5 h. Under moderately acidic conditions representative of aerosol particles (pH = 3−4), the decarboxylation rate increased linearly with ammonium concentration up to about 2.7 M, after which additional ammonium had no effect. The effective lifetime of OAA reduced to approximately 1 h under these conditions. Density functional theory calculations support the proposed catalytic mechanism, predicting the free energy barrier height for decarboxylation to be approximately 21 kcal/mol lower after OAA has reacted with ammonium. In more acidic solutions (pH < 1), OAA's decarboxylation was suppressed, with lifetimes of tens of hours, even in the presence of ammonium. A comparison of the decarboxylation rate with the expected rate of oxidation by OH suggests that decarboxylation will be the dominant loss mechanism for OAA, and presumably other 3-oxocarboxylic acids, in aerosol particles and cloud/fog droplets. This result explains why OAA is hard to detect in field measurements even though it is a known oxidation product of succinic acid.

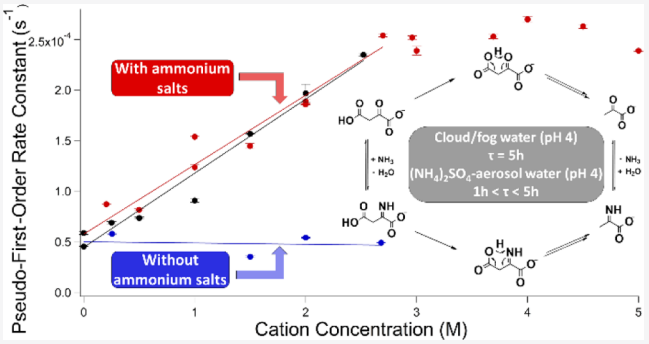

KEYWORDS: *decarboxylation, ammonium catalysis, acidity, secondary organic aerosol, chemical aging*

INTRODUCTION

The importance of secondary organic aerosol (SOA) formation and aging has been recognized based on SOA's ability to affect climate, air quality, and health.[1] SOA is generally comprised of molecules containing carbonyl, carboxyl, and hydroxyl functional groups.[2] Oxocarboxylic acids and dicarboxylic acids comprise a major fraction of SOA mass as a result of their low vapor pressures.[3] Their abundance in atmospheric water is also high as a result of their high polarity.[4] Their prevalence in SOA and water solubility makes dicarboxylic acids, oxocarboxylic acids, and oxodicarboxylic acids (molecules that have two carboxyl groups and at least one keto group) good representative molecules for SOA found in the aqueous phase, such as aerosol liquid water or cloud droplets, and studying their possible aqueous reactions is important for understanding the fate of SOA molecules dissolved in atmospheric water.[3,5−12]

The ionic strengths for atmospheric water generally fall between 10^{-5} and 10^{-2} M for cloud/fog water and in excess of 1 M in deliquescent aerosol particles.[8] The major contributors to the ionic strength are sulfate and ammonium ions, especially in areas dominated by anthropogenic emissions of ammonia and sulfur dioxide,[5] but other inorganic ions including nitrate, chloride, and sodium also contribute. These hygroscopic species have the potential to affect the chemistry of SOA in the aqueous phase through various mechanisms. Ammonium ions are especially interesting in this regard because they directly affect the pH, and they can act as a catalyst for various processes by reacting with carbonyl and other oxygen-containing groups.[13,14] One such ammonium-catalyzed process is the main focus of this work.

Oxaloacetic acid (OAA) is a 3-oxodicarboxylic acid—a class of compounds, which are known to undergo the decarbox-

Received: January 28, 2021
Revised: March 9, 2021
Accepted: March 16, 2021
Published: March 25, 2021

ylation reaction shown in simplified Scheme 1. OAA can be formed by the oxidation of succinic acid,[15] which is prevalent in the atmosphere,[9,12] and OAA has recently been observed in atmospheric aerosols.[6,7,16] Previously, the decarboxylation reaction of 3-oxocarboxylic acids has been suggested by Römpp et al.[11] to explain the absence of 3-oxodicarboxylic acids detected in field data, despite their assumed formation and detection in laboratory-generated SOA. In fact, it has been known for some time that OAA's decarboxylation reaction can be catalyzed by ammonium and other amines.[17] Because OAA is an important molecule in the citric acid cycle,[18] this decarboxylation reaction and response to ammonium and amines has been reported in previous studies, usually under more neutral or basic conditions and ionic strengths and temperatures more representative of the human body.[19−22] The behavior of OAA under the higher ionic strength conditions of deliquescent aerosol particles has not been studied.

Scheme 1. Decarboxylation Reaction of OAA[a]

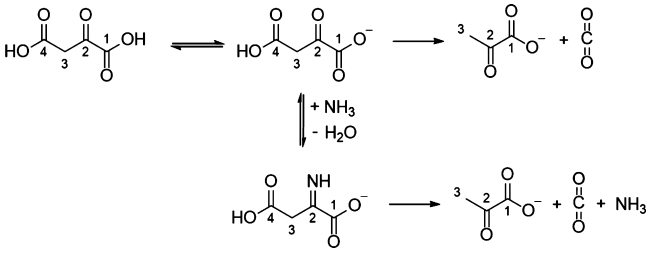

[a]The mechanism is based on Thalji et al.[22] The reaction is adjusted to represent the majority species at pH 3 to 4 by not deprotonating the carboxylic acid at carbon 4. The p*K*3 of the carboxylic acid at carbon 1 is 2.15 and the pK_a of the carboxylic acid at carbon 4 is 4.06.[23] The reaction is catalyzed by forming an imine as shown here.

The ammonium-catalyzed decarboxylation of OAA has not been studied with theoretical methods. Previous theoretical calculations have provided many mechanistic insights into catalysis of reaction by diamines, although with the important limitation that they do not exhaustively explore possible decarboxylation pathways. Song et al.[24] reported a detailed mechanism and proton-transfer pathway for the uncatalyzed and ethylenediamine-catalyzed decarboxylation of undissociated OAA in the gas phase and aqueous phase proposed using semilocal density functional theory (DFT). They found an uncatalyzed free energy barrier of about 24 kcal/mol and an ethylenediamine-catalyzed free energy barrier of approximately 14 kcal/mol, and the dehydration of the carbinolamine to form an imine was the rate-limiting step for the catalyzed reaction. A detailed mechanism for fully deprotonated OAA at pH 8.0 with and without catalysis by protonated ethylenediamine was calculated by Cheng.[25] When fully deprotonated, the dehydration of the carbinolamine was still the rate-limiting step, but the free energy barrier was greater: 49 kcal/mol with ethylenediamine catalysis (the free energy barrier and the rate-limiting step without a catalyst were not discussed). Finally, Fan and Song[26] used DFT to compare several protonated diamine catalysts in the decarboxylation of OAA's anions (OAA^- and OAA^{2-}). They calculated the decarboxylation step to have the highest free energy for OAA^{2-} in the presence of all diamine catalysts, while the dehydration of the carbinolamine was rate-determining for OAA^- with most of the catalysts.

We have examined the chemistry of OAA in the presence of varying, atmospherically relevant concentrations of NH_4^+ and SO_4^{2-}, as well as Na^+ and Cl^- for comparison, which simulate a number of aqueous conditions found in the atmosphere. We also report electronic structure calculations in order to generate the energy diagrams of both the uncatalyzed and ammonium-catalyzed decarboxylation of OAA. We propose that the ammonium-catalyzed reaction goes through a six-membered ring transition state, which is analogous to the known transition state of the uncatalyzed reaction, as presented in Scheme 2. We compare the activation energies of both mechanisms to validate our experimental results. We show that decarboxylation in the presence of ammonium occurs on time scales of hours, and therefore controls the lifetime of OAA, and likely all other 3-oxocarboxylic acids, in the presence of ammonium sulfate aerosols.

MATERIALS AND METHODS

Sample Aging. OAA (97% purity) was purchased from Millipore Sigma. Ammonium sulfate (99% purity), ammonium bisulfate (98% purity), ammonium chloride (99% purity), and sodium sulfate (99% purity) were purchased from Fisher Scientific. All compounds were used without further purification. OAA was dissolved in pure Milli-Q water or solutions of varying concentrations of ammonium sulfate, ammonium bisulfate, sodium sulfate, or ammonium chloride to make 1 mM solutions of OAA. The OAA dissolved promptly upon contact with the solution, so minimal mixing was required. The time between solution preparation and the beginning of measurements was minimized (<5 min) to control the amount of time spent in the aqueous phase, allowing for the observation of as much of the decarboxylation reaction as possible. The rate of the decarboxylation reaction shown in Scheme 1 was monitored using the peak in absorbance at 260 nm using a UV−vis spectrometer (Shimadzu UV-2450), which was programmed to collect a spectrum at set time intervals, ranging from 10 to 30 min depending on the rate at which the absorbance decayed. The 1

Scheme 2. Proposed Mechanism for OAA's Decarboxylation Including the Six-Membered Ring Transition State (a) without Catalyst and (b) in the Presence of Ammonium

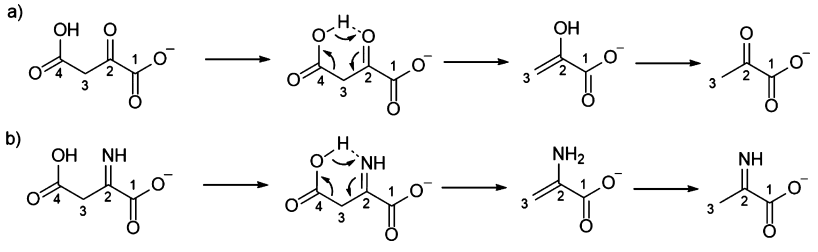

https://doi.org/10.1021/acsearthspacechem.1c00025
ACS Earth Space Chem. 2021, 5, 931−940

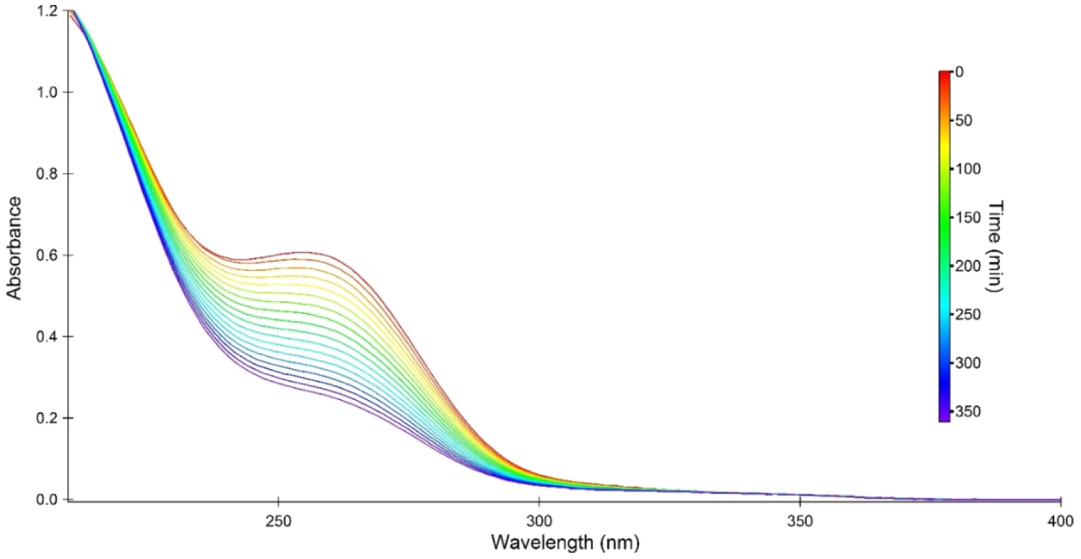

Figure 1. Absorption spectrum of OAA in water over time. The spectrum shows a peak at 260 nm, which decays with a first-order rate constant of $(5.91 \pm 0.15) \times 10^{-5}$ s^{-1} for the trial shown, giving OAA a lifetime of about 5 h with respect to decarboxylation in the absence of ammonium ions or other catalysts.

mM OAA concentration was specifically chosen to provide a starting 260 nm absorbance around one to ensure a good signal-to-noise ratio. We did not vary the starting concentration in these experiments since OAA exhibited first-order decay. The pH value for each starting sample was measured using a Mettler Toledo SevenEasy pH meter. The pH of the solutions did not change significantly throughout the experiments, which agrees with previous work.[27,28]

Rate Constant and Branching Ratio Calculations. Rate constants and standard deviations were determined by fitting the absorbance at 260 nm over time to a first-order rate law. Sample fits to the data are shown in Figures S1−S3. The decarboxylation reaction has also been shown to be of first order in previous studies.[21,29]

To determine the importance of the decarboxylation reaction relative to other loss processes, the measured rate constants were converted into lifetimes with respect to decarboxylation, and compared to calculated lifetimes with respect to oxidation by OH using the method described in ref 30. We define Q below as the ratio of the rate of oxidation of OAA by OH to the rate of decarboxylation

$$Q = \frac{\tau_d}{\tau_{OH}} = \frac{k_{OH}[OH]}{k_d} \quad (1)$$

where τ_d is the lifetime of OAA with respect to decarboxylation, τ_{OH} is the lifetime of OAA with respect to OH oxidation, k_{OH} is the bimolecular rate constant for OAA's reaction with OH, and k_d the measured unimolecular rate constant for OAA's decarboxylation. OH concentrations for deliquescent particles and cloud/fog water have been estimated to be 10^{-16} to 10^{-15} M.[31−33] Therefore, for the purposes of this comparison, the OH concentration was assumed to be 10^{-15} M for most of the discussion, although the implications of higher OH concentrations are addressed briefly.

The reaction rate of OAA with the OH radical has not been previously determined, so the structure−activity relationships (SARs) for aqueous OH-oxidation developed by Monod and Doussin[34,35] were used to estimate k_{OH} for OAA. OAA has multiple acid−base sites and can form a *gem*-diol or enol in the aqueous phase, so the mixture of compounds contributing to its OH reactivity is complex. Equilibrium ratios of all possible forms of OAA present in aqueous solutions at various pH values were previously determined by Kozlowski and Zuman[20] and were used here to determine a weighted rate constant for the OH-oxidation of OAA. The rate constants for the OH-oxidation of unsaturated compounds were not included in the SARs' training data set,[34,35] so the enol forms of OAA could not be calculated. Instead, the OH-oxidation rate of the closely related but-2-enedioic acid was used to estimate the OH reactivity of the enol forms of OAA (for equilibrium ratios and more details on OH-oxidation calculations, see Tables S2 and S3).

Computational Details. To further analyze our experimental results, we performed electronic structure calculations to obtain the energy diagrams for both the uncatalyzed and ammonium-catalyzed decarboxylation of OAA. The main goal of these simulations was to establish the mechanism for decarboxylation, rather than quantitatively predict the rate constants, using resource-efficient computational methodology. Geometries of the reactants, transition-state intermediates, and products were fully optimized within DFT using the hybrid exchange−correlation functional of Perdew, Burke, and Ernzerhof (PBE0)[36] in combination with the resolution-of-identity approximation.[37] PBE0 has been shown to give acceptably accurate barrier heights based on previous work,[30] so in the interest of computational cost, other hybrid exchange−correlation functionals were not tested. Polarized triple-zeta valence basis sets (def2-TZVPP)[38] were used for all atoms. Very fine size four[39] (grids) was used for numerical integration, and ground-state energies converged to 10^{-8} hartree. Analytical second derivative (AOFORCE)[40] calculations were performed to confirm that all optimized structures were minima of the potential energy surface. In addition to doing calculations for isolated molecules, we also performed calculations for molecules in a dielectric medium. To this end, the conductor-like screening model (COSMO)[41] was employed with the dielectric constant for water, 80.1.[42] For

https://doi.org/10.1021/acsearthspacechem.1c00025
ACS Earth Space Chem. 2021, 5, 931−940

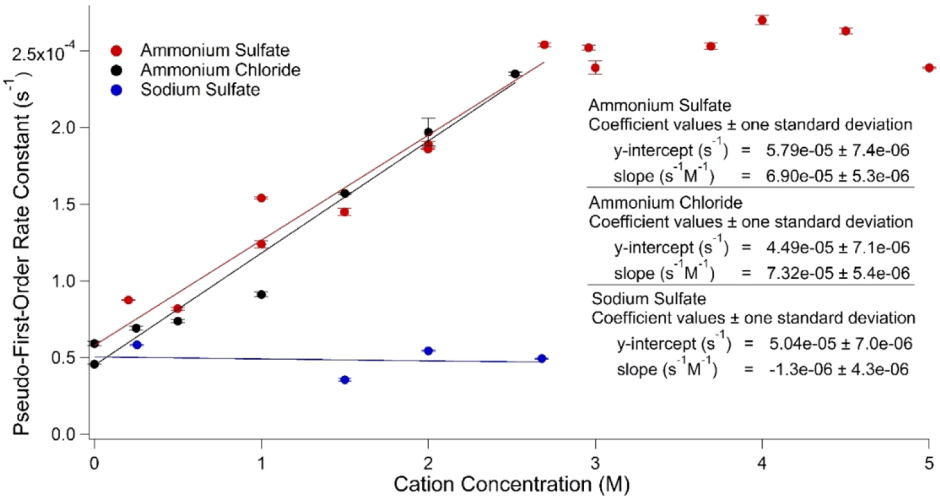

Figure 2. Pseudo-first-order rate constants for the decay of OAA's absorbance peak at 260 nm as a function of cation concentration (ammonium concentration for ammonium sulfate and ammonium chloride; sodium concentration for sodium sulfate). The data for ammonium sulfate are shown in red, ammonium chloride in black, and sodium sulfate in blue. Error bars represent standard deviations computed from the individual fits. As the temperature and pH were not intentionally fixed, some spread in the rate constants obtained may be expected due to variations in the room temperature or differences in the solution pH. This particularly applies when comparing the ammonium sulfate (pH = 3.7 ± 0.3) and ammonium chloride conditions (pH = 3.0 ± 0.3). See Table S1 for more detailed information on the pH of individual experimental trials.

each proposed mechanism, a search for transition states was performed by scanning the ground-state potential energy surface along the carbon C_3-C_4 bond distance, followed by an unconstrained transition state optimization. The validity of the transition state structures was checked using numerical finite differences of analytical gradients[43] to ensure there was one imaginary frequency. The Gibbs free energies of each species within the rigid-rotor harmonic oscillator approximation at 25 °C and 1 atm were subsequently calculated. Energy diagrams for OAA's decarboxylation were generated by setting the reference energy of all the reactants to zero. All electronic structure calculations were carried out with the TURBOMOLE electronic structure program suite, version V7.3.[44]

RESULTS AND DISCUSSION

Uncatalyzed Decarboxylation. Decarboxylation of OAA occurs slowly in pure water, and we remeasured the rate of this process in control experiments. The change in the absorbance spectrum over time can be seen in Figure 1. We determined the uncatalyzed rate constant for the decarboxylation to be $(5.24 \pm 0.95) \times 10^{-5}$ s^{-1} as an average and standard deviation of two measurements, which shows good agreement with previous work (5.5×10^{-5} s^{-1}).[20] This gives OAA a lifetime of about 5 h in a dilute aqueous solution, such as a cloud droplet. This is more than two orders of magnitude shorter than the lifetime with respect to the oxidation by OH in cloud/fog water (predicted $Q = 0.005$), so decarboxylation will be the major removal pathway for aqueous OAA under these conditions.

Effects of Ammonium in Weakly Acidic Solutions (pH 3 to 4). The measured pseudo-first-order rate constants (k) and their dependence on salt concentrations are shown in Figure 2. Here, we plot the rate constants as a function of cation (ammonium or sodium) concentration rather than the overall ionic strength because we observe that ammonium ion concentration better correlates with changes in the observed rate constants. An increase in ammonium sulfate linearly increases the rate constant for the decarboxylation reaction, with a slope of about 7×10^{-5} s^{-1} per molar ammonium. The dependence of the rate on ammonium concentration appears to reach an asymptote above about 2.7 M ammonium. The lifetime of OAA at the point the rate levels off is about 1 h. We have confirmed using the E-AIM model II (http://www.aim.env.uea.ac.uk/aim/aim.php) that the activity of ammonium ion increases smoothly with ammonium sulfate concentration over this concentration range, so the saturation above 2.7 M is not due to the changes in the activity of ammonium ions.

Figure 2 compares the measured rate constant for both ammonium sulfate and ammonium chloride. The dependence of the measured rate constant on the ammonium ion concentration is the same regardless of whether the sulfate or chloride salt of ammonium is used, so there are no strong anion effects on decarboxylation. Control experiments were performed based on previous work, which has shown some atmospheric aqueous processes to be influenced by ionic strength.[8,45−47] However, the rate constant for decarboxylation does not show a dependence on the salt concentration with the addition of sodium sulfate. While we do not plot the data as a function of ionic strength in Figure 2, the ionic strength increases with increasing sodium sulfate concentration, so we can conclude that the reaction is not appreciably affected by ionic strength in this case.

We can explain the observed behavior of the effective rate constant on $[NH_4^+]$ if we assume that ammonia present in solution converts a small fraction of the carbonyl species into imine (Scheme 1), which then decarboxylates at a much higher rate (Scheme 2). The measured relative rate of decarboxylation in the presence and absence of dissolved ammonia in the limit of a rapid imine−carbonyl equilibrium can be expressed as follows

$$\frac{\text{rate}_{\text{with NH}_3}}{\text{rate}_{\text{without NH}_3}} = \frac{k_{\text{imine}}[\text{imine}] + k_{\text{carbonyl}}[\text{carbonyl}]}{k_{\text{carbonyl}}[\text{carbonyl}]} \approx 1 + \frac{k_{\text{imine}}K_{\text{eq}}[\text{NH}_3]}{k_{\text{carbonyl}}} \quad (2)$$

https://doi.org/10.1021/acsearthspacechem.1c00025
ACS Earth Space Chem. 2021, 5, 931−940

Here, [carbonyl] is the starting concentration of OAA, [imine] is the concentration of imine assumed to be a minority species in solution ([imine] ≪ [carbonyl]), $k_{carbonyl}$ is the rate constant for decarboxylation from the carbonyl species (measured to be 5.24×10^{-5} s^{-1}), k_{imine} is the unknown rate constant for decarboxylation from the imine species, and K_{eq} is the equilibrium constant between the imine and carbonyl species.

$$K_{eq} = \frac{[\text{imine}]}{[\text{carbonyl}][NH_3]} \quad (3)$$

Ammonia is a minor species in solution under acidic conditions, but its concentration can be calculated from the acid ionization constant K_a of the ammonium ion

$$K_a = \frac{[H_3O^+][NH_3]}{[NH_4^+]} = 5.6 \times 10^{-10} \quad (4)$$

Combining these equations results in a predicted proportionality of the relative decarboxylation rate on the ammonium ion concentration

$$\frac{\text{rate}_{\text{with } NH_3}}{\text{rate}_{\text{without } NH_3}} = 1 + \frac{k_{imine}K_{eq}}{k_{carbonyl}} \times \frac{K_a[NH_4^+]}{[H_3O^+]} \quad (5)$$

This can be related to the pseudo-first-order rate constant shown in Figure 2

$$k_{effective} = k_{carbonyl} + k_{imine}K_{eq} \times \frac{K_a[NH_4^+]}{[H_3O^+]} \quad (6)$$

which is consistent with the observed linear dependence on $[NH_4^+]$ below $[NH_4^+] \approx 2.7$ M. The linearity breaks down at higher concentrations, likely because the equations of equilibrium, eqs 3 and/or 4, no longer work at high ionic strengths. It is also possible that our assumption of the rapid equilibrium between imine and carbonyl is not valid, which would contribute to the nonexponential decay of absorbance shown in Figures S1−S3.

Effects of Ammonium in Highly Acidic Solutions (pH near or Less Than 1). Pseudo-first-order rate constants were also measured for solutions of OAA with varying concentrations of ammonium bisulfate, shown in Table 1. These

Table 1. Data from Individual Decarboxylation Reactions in the Presence of Ammonium Bisulfate

ammonium bisulfate concentration (M)	solution pH	rate constant (s^{-1})	lifetime (h)
0 (H_2SO_4 added)	1.0	$(4.36 \pm 0.04) \times 10^{-6}$	63.7
0.5	1.3	$(8.05 \pm 0.12) \times 10^{-6}$	35.5
0.8	1.0	$(6.15 \pm 0.10) \times 10^{-6}$	45.2
1.5	0.4	$(4.49 \pm 0.03) \times 10^{-6}$	62.0
2.0	0.2	$(2.37 \pm 0.04) \times 10^{-6}$	117

experiments showed much slower rates of decarboxylation. At these low pH values, there is a strong contribution by the *gem*-diol form of OAA,[20] which should decrease the decarboxylation rate because the most likely reaction intermediate requires the keto form.[24] In addition, the rate is suppressed by the low concentration of ammonia needed to produce the imine, resulting in anticorrelation between the effective rate constant and the hydronium ion concentration (eq 6). As a control experiment, we measured the decarboxylation rate of OAA in an aqueous solution acidified to pH 1.0 with sulfuric acid in the absence of ammonium and found a lifetime of 63.7 h. This is longer than for the solution containing ammonia at the same pH 1.0 (45.2 h), showing that ammonia does still catalyze the decarboxylation even at these highly acidic pHs. However, the catalytic effect of ammonia is not strong enough to counteract the suppression of the decarboxylation rate by the increased acidity.

Although the *gem*-diol reacts more readily with the OH radical than the keto form of OAA, decarboxylation is still the faster process at an OH concentration of 10^{-15} M, with branching ratio Q ranging from 0.042 for 0.5 M ammonium bisulfate to 0.14 for 2.0 M ammonium bisulfate. If particle OH concentrations are higher, for instance 10^{-12} M as suggested by Ervens et al. in their 2011 review,[48] OH oxidation lifetimes would be much shorter, and the branching ratios would shift to 42 for 0.5 M ammonium bisulfate and 140 for 2.0 M ammonium bisulfate. The importance of OAA's decarboxylation reaction will, therefore, be highly OH-concentration dependent under acidic conditions, as acidity greatly decreases the decarboxylation rate.

Electronic Structure Calculations. Two possible reaction pathways for the ammonium-catalyzed decarboxylation of OAA are presented in Figure 3, one starting from the imine

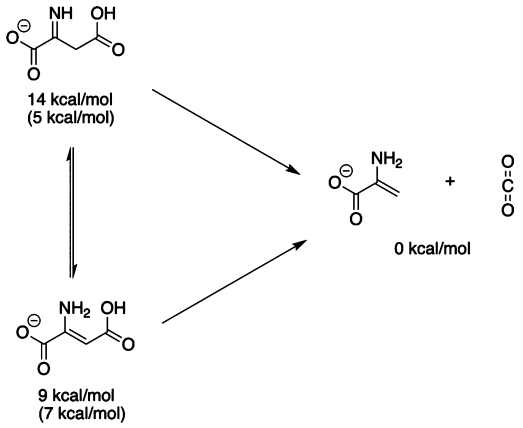

Figure 3. Electronic energies of species likely involved in the ammonium-catalyzed decarboxylation of OAA. The reference energy of the product was set to 0 kcal/mol, and the reference energy of the imine and enamine species were calculated accordingly. Values without and with parentheses are the relative free energies in the aqueous phase and the gas phase, respectively. All energies were calculated at the PBE0/TZVPP level and reported in kcal/mol.

form and one starting from the enamine form of the reaction intermediate. Because most of our experiments were conducted at pH 3 to 4, which is higher than the pK_a at carbon 1 and lower than the pK_a at carbon 4, we began our simulations with the monodeprotonated form of OAA as this should be the majority species in solution. To determine which of these pathways is more thermodynamically favorable, the stability of both compounds was compared to that of the decarboxylation enamine product. In the gas phase, the starting enamine species has a lower free energy (5 kcal/mol) than the imine (7 kcal/mol) relative to the product. However, the energy order switches in the aqueous phase (14 kcal/mol for the imine vs 9 kcal/mol for the enamine). In both the gas and aqueous phases, the reaction is predicted to be exergonic.

Figure 4 shows the energy diagrams for the ammonium-catalyzed and uncatalyzed decarboxylation processes in the gas

https://doi.org/10.1021/acsearthspacechem.1c00025
ACS Earth Space Chem. 2021, 5, 931−940

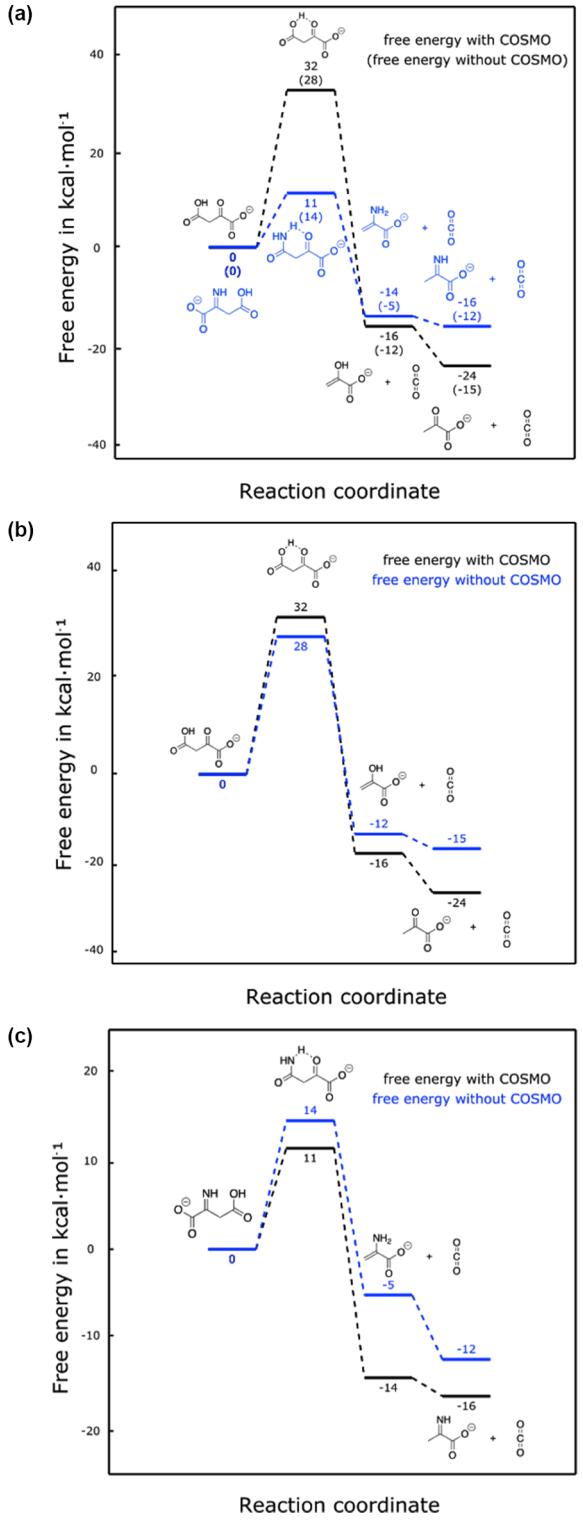

Figure 4. (a) Select stationary points of the uncatalyzed (black) and ammonium-catalyzed (blue) decarboxylation reaction of OAA. Values without and with parentheses are the relative free energies with COSMO (representing the aqueous phase) and without COSMO (representing the gas phase), respectively. (b) Select stationary points of the uncatalyzed decarboxylation of OAA without COSMO (gas phase) shown in blue and with COSMO (aqueous phase) shown in black. (c) Select stationary points of the ammonium-catalyzed decarboxylation of OAA without COSMO (gas phase) shown in blue and with COSMO (aqueous phase) shown in black. All energies were calculated at the PBE0/TZVPP level and reported in kcal/mol.

and aqueous phases. Our calculations found the transition state for the uncatalyzed decarboxylation is stabilized by the formation of a six-membered ring as shown in Scheme 2 and Figure 4, in agreement with previous theoretical studies on the uncatalyzed decarboxylation of OAA and related molecules.[24,49,50] Our calculated activation energy of 32 kcal/mol for the aqueous phase uncatalyzed reaction is higher than the experimentally determined activation energy of 23.6 kcal/mol reported by Ito et al.,[27] but still within a range expected of our lower target accuracy. Our calculated energy barriers may be high because we did not allow for tunneling in our calculations. In the catalyzed reaction, the decarboxylation proceeds from the imine form, and an analogous six-membered ring is formed for the ammonium-catalyzed transition state (also shown in Figure 4). The activation energy of the ammonium-catalyzed decarboxylation is significantly lower than that of the uncatalyzed decarboxylation in both the gas and aqueous phases, which is consistent with our relative experimental decarboxylation rates. Replacing OAA's carbonyl with an imine lowers the activation energy for decarboxylation, leading to shorter lifetimes in solutions containing ammonium. Comparing the gas and aqueous phase energy levels, it can also be seen from Figure 4 that the solvation effect of water stabilizes all the species except for the uncatalyzed transition state.

We used the Curtin–Hammett principle to calculate the relative free energies of the transition states ($\Delta\Delta G^{\ddagger}$).[51]

$$\Delta\Delta G^{\ddagger} = \Delta G^{\ddagger}_{\text{carbonyl}} - \Delta G^{\ddagger}_{\text{imine}} + \Delta G^{\circ}_{\text{eq}} \tag{7}$$

$\Delta G^{\ddagger}_{\text{carbonyl}}$ and $\Delta G^{\ddagger}_{\text{imine}}$ are the activation energies for decarboxylation from the carbonyl and imine, and $\Delta G^{\circ}_{\text{eq}}$ is the free energy of the carbonyl and imine equilibrium (assumed to be achieved faster than the time scale of the decarboxylation process). The gas-phase theoretical value of $\Delta\Delta G^{\ddagger}$ is 14 kcal/mol. Calculating $\Delta\Delta G^{\ddagger}$ while including the dielectric constant of water to represent the aqueous phase gives 24 kcal/mol.

The Curtin–Hammett principle also makes it possible to estimate $\Delta\Delta G^{\ddagger}$ from our experimental results using the following equation

$$\frac{k_{\text{imine}}K_{\text{eq}}}{k_{\text{carbonyl}}} = e^{\Delta\Delta G^{\ddagger}/RT} \tag{8}$$

Using eq 6, we determined $k_{\text{imine}}K_{\text{eq}}$ = 12.5 at pH of 4 (see Table S1 for experimental pH values) from the experimentally determined slope in Figure 2. Inserting this value into eq 8, along with the measured k_{carbonyl} rate constant, gave us an experimental $\Delta\Delta G^{\ddagger}$ value of about 7.3 kcal/mol. The experimentally derived value is considerably lower than the theoretical value suggesting that the calculation overestimates the barrier height for the carbonyl species (by about 8 kcal/mol as discussed above) but underestimates the barrier height for the imine species. It is also possible that other forms of OAA shown in Scheme 2 can decarboxylate making the direct comparison between the theory and experiment more challenging. Despite these quantitative discrepancies, which may in part be due to the neglect of proton tunneling on the computed barriers, the computations support the experimental observations by suggesting that the decarboxylation reaction proceeds more efficiently along the catalyzed pathway due to a lower transition-state energy along this pathway.

Effect of Ionic Strength on the Initial Absorbance Spectra. It has been demonstrated that increasing salt

https://doi.org/10.1021/acsearthspacechem.1c00025
ACS Earth Space Chem. 2021, 5, 931–940

concentrations can affect the absorption spectra of aqueous molecules and impact their direct photolysis rates.[45,46,52,53] This prompted us to examine the effect of the added salts on the initial absorption spectrum of OAA before the decarboxylation (Figures S4−S7).

Under all conditions, the addition of small concentrations (less than 1 M) of salts resulted in an increase in the height of the main absorption peak at 260 nm. However, further addition of salt decreased the 260 nm absorption. The decrease holds true for the solutions containing sodium sulfate as well as for the solutions containing ammonium, so we do not believe it is attributable to faster decarboxylation with ammonium. This effect was not observed in previous studies on pyruvic acid[45,52] (another atmospherically important keto-acid and the product of the OAA decarboxylation) and is likely a result of changing OAA's complex equilibrium of species in solution. Since the enol form is the major absorbing species for OAA,[20] any change in the enol concentration will change the absorption intensity. Other single-molecule experiments have shown that salts can affect the absorbance spectra by changing the ratios of species present in solution,[46,52] although these other studies have been on molecules with a less complex set of forms at equilibrium. A decrease in the relative enol concentration explains why lowering the pH of the solutions (under ammonium bisulfate and sulfuric acid conditions) significantly decreased the main absorption peak, as there is a greater fraction of *gem*-diol and a lower fraction of enol present under acidic conditions.[20] An additional consequence of increased acidity is reduced absorption above 300 nm. OAA will absorb less of the sun's energy under very acidic conditions (pH near or less than 1) than at more moderately acidic pHs, which may affect its photochemistry.

Another interesting effect is the growth of a shoulder on the main absorption peak with the addition of ammonium sulfate (Figure S4), providing more absorption of tropospherically relevant wavelengths. This shoulder, characterized by an increase in absorbance between 270 and 315 nm, is attributable to the formation of an enamine,[54] which would be particularly interesting if the enamine form is not active in the decarboxylation process as could be the case based on our and previous calculations.[24−26] Therefore, enamine formation may be a potential pathway for direct photolysis to compete with OAA's decarboxylation. The enamine peak is only visible at pH values above about 3.5, as demonstrated by the ammonium chloride-containing absorbance spectra (Figure S6). Since ammonium chloride is more acidic than ammonium sulfate or sodium sulfate, the ammonium chloride solutions were generally near pH 3 and the enamine peak was not present. However, when a drop of 1 N potassium hydroxide was added to the sample solution, the pH changed from ∼3 to ∼4 and the enamine band became visible. It is clear from the comparison of the initial absorbance spectra that pH, ionic strength, and ionic species can alter the absorption spectrum of OAA significantly, and potentially affect its direct photolysis rate.

CONCLUSIONS

The decarboxylation rate of OAA was observed in solutions of ammonium and sulfate salts at varying concentrations and compared to the reaction rate in pure water, and electronic structure calculations were performed to validate our experimental results. At weakly acidic pH values, the rate at which OAA was converted to pyruvic acid linearly increased with the addition of ammonium up to about 2.7 M ammonium but had no further observable change in the rate at higher ammonium concentrations. At pH values near and less than 1, the decarboxylation reaction rate was reduced by about an order of magnitude, although ammonium still catalyzed the reaction. Salts that did not contain ammonium did not accelerate the observed reaction. The DFT calculations performed suggest that the energy barrier for decarboxylation is significantly lower from the imine (after reaction with ammonium) than from the uncatalyzed carbonyl form: 11 kcal/mol compared to 32 kcal/mol.

When decarboxylation lifetimes were compared to the lifetimes of OAA with respect to OH oxidation under corresponding atmospheric conditions, decarboxylation was found to be dominant for nearly all cases. These results suggest that the lifetime of OAA will be highly dependent on the aqueous system in which it is dissolved. In dilute solutions (such as cloud water) and aerosols with low ammonium concentrations, decarboxylation reactions of the type studied here will be ammonium (or amine) concentration-dependent, but the exact ammonium concentration will not be as important in deliquescent particles in cases where the ammonium concentration is sufficiently high. At highly acidic pH values, the importance of decarboxylation will depend on the OH concentration, but decarboxylation is still likely to be the dominant removal pathway. The decarboxylation lifetimes calculated here can be summarized as follows: 5 h in dilute water/weakly acidic water without ammonium ions, less than 5 h and as short as 1 h in water neutralized by ammonium, and tens of hours in more acidic waters.

Decarboxylation and OH oxidation do not exhaustively describe all possible fates for OAA in atmospheric water. For instance, reactions between carboxylic acids and ammonium or protonated amines have been shown to contribute to nanoparticle growth.[55] Formation of a carboxylate salt of this type with the carboxylic acid at OAA's carbon 4 would inhibit the decarboxylation pathway shown in Scheme 2, suppressing decarboxylation in freshly nucleated particles. Sulfate-esterification may also occur in sulfate-containing atmospheric solutions, particularly at low pH values.[56] The methods presented here do not allow us to differentiate sulfate-esterification from decarboxylation under our highly acidic conditions where sulfate-esterification is expected to gain importance. However, formation of sulfate esters has been shown to result from the reactions of epoxides, while their formation from the reactions of alcohols (e.g., the enol form of OAA) is kinetically unfavorable under atmospheric conditions.[57,58] Finally, small ketone-containing molecules can undergo aldol condensation catalyzed by the presence of ammonium,[59] which could also compete with decarboxylation. The rate of aldol condensation has not been measured for OAA, so we cannot directly compare the lifetimes of OAA with respect to decarboxylation and aldol condensation. However, rates of aldol condensation for other small carbonyl compounds are on the order of 10^{-5} to 10^{-7} s^{-1}—one to three orders of magnitude slower than the decarboxylation of OAA is predicted to be under similar conditions.[13] We, therefore, expect decarboxylation to be the most important process for OAA in atmospheric particles containing ammonium.

We also expect decarboxylation to be an important removal pathway for other 3-oxocarboxylic acids, although the reactivity of OAA may not translate directly. Other 3-oxocarboxylic

https://doi.org/10.1021/acsearthspacechem.1c00025
ACS Earth Space Chem. 2021, 5, 931−940

acids, such as acetoacetic acid and α,α-dimethylacetoacetic acid, have decarboxylation rates of the same order of magnitude as OAA in pure water,[60,61] and we expect ammonium salts to catalyze the decarboxylation reactions of other molecules similarly. However, the OH reactivity of these other molecules may differ from OAA. OAA has an especially unreactive keto form as a result of its structure (it only has one carbon where hydrogen atoms can be abstracted by OH radicals). However, it also has a strong tendency to form a *gem*-diol (which reacts more quickly with OH) and exists as an enol in small abundances (which reacts very readily with OH). Other molecules will likely have a more OH-reactive keto form, be less likely to form a *gem*-diol, and may not have an enol form. It will be useful for future work to determine if/how the structure of 3-oxocarboxylic acids affects the ammonium-catalyzed decarboxylation, and if OH oxidation becomes more important than decarboxylation for other 3-oxocarboxylic acids.

■ ASSOCIATED CONTENT

Supporting Information

The Supporting Information is available free of charge at https://pubs.acs.org/doi/10.1021/acsearthspacechem.1c00025.

More detailed experimental data, details of OH oxidation rates and branching ratio calculations, sample fits of decarboxylation curves, $t = 0$ absorbance spectra under all conditions discussed in this work, and coordinate file information for the optimized geometries (PDF)

■ AUTHOR INFORMATION

Corresponding Author

Sergey A. Nizkorodov − *Department of Chemistry, University of California, Irvine, Irvine, California 92697, United States;* orcid.org/0000-0003-0891-0052; Email: nizkorod@uci.edu

Authors

Alexandra L. Klodt − *Department of Chemistry, University of California, Irvine, Irvine, California 92697, United States;* orcid.org/0000-0002-3558-972X

Kimberly Zhang − *Department of Chemistry, University of California, Irvine, Irvine, California 92697, United States*

Michael W. Olsen − *Department of Chemistry, University of California, Irvine, Irvine, California 92697, United States*

Jorge L. Fernandez − *Department of Chemistry, University of California, Irvine, Irvine, California 92697, United States*

Filipp Furche − *Department of Chemistry, University of California, Irvine, Irvine, California 92697, United States;* orcid.org/0000-0001-8520-3971

Complete contact information is available at: https://pubs.acs.org/10.1021/acsearthspacechem.1c00025

Author Contributions

The experiments and data analysis were conceived by S.A.N. and A.L.K. and carried out by J.L.F., M.W.O., and A.L.K. The calculations were conceived by K.Z. and F.F. and done by K.Z. The manuscript was written by A.L.K. with contributions from all the coauthors. All authors have given approval to the final version of the manuscript.

Notes

The authors declare no competing financial interest.

■ ACKNOWLEDGMENTS

Experiments reported in this work were supported by the US National Science Foundation grant AGS-1853639. Electronic structure calculations were supported by the US National Science Foundation grant CHE-1800431. K.Z. was supported by the Beckman Scholars Program from the Arnold and Mabel Beckman Foundation.

■ REFERENCES

(1) Pöschl, U. Atmospheric Aerosols: Composition, Transformation, Climate and Health Effects. *Angew. Chem., Int. Ed.* **2005**, *44*, 7520−7540.

(2) Atkinson, R.; Arey, J. Atmospheric Degradation of Volatile Organic Compounds. *Chem. Rev.* **2003**, *103*, 4605−4638.

(3) Saxena, P.; Hildemann, L. M. Water-Soluble Organics in Atmospheric Particles: A Critical Review of the Literature and Application of Thermodynamics to Identify Candidate Compounds. *J. Atmos. Chem.* **1996**, *24*, 57−109.

(4) Fuzzi, S.; Facchini, M. C.; Decesari, S.; Matta, E.; Mircea, M. Soluble Organic Compounds in Fog and Cloud Droplets: What Have We Learned over the Past Few Years? *Atmos. Res.* **2002**, *64*, 89−98.

(5) Bikkina, S.; Kawamura, K.; Sarin, M. Secondary Organic Aerosol Formation over Coastal Ocean: Inferences from Atmospheric Water-Soluble Low Molecular Weight Organic Compounds. *Environ. Sci. Technol.* **2017**, *51*, 4347−4357.

(6) Gowda, D.; Kawamura, K.; Tachibana, E. Identification of Hydroxy- and Keto-Dicarboxylic Acids in Remote Marine Aerosols Using Gas Chromatography/Quadruple and Time-of-Flight Mass Spectrometry. *Rapid Commun. Mass Spectrom.* **2016**, *30*, 992−1000.

(7) Gowda, D.; Kawamura, K. Seasonal Variations of Low Molecular Weight Hydroxy-Dicarboxylic Acids and Oxaloacetic Acid in Remote Marine Aerosols from Chichijima Island in the Western North Pacific (December 2010−November 2011). *Atmos. Res.* **2018**, *204*, 128−135.

(8) Herrmann, H.; Schaefer, T.; Tilgner, A.; Styler, S. A.; Weller, C.; Teich, M.; Otto, T. Tropospheric Aqueous-Phase Chemistry: Kinetics, Mechanisms, and Its Coupling to a Changing Gas Phase. *Chem. Rev.* **2015**, *115*, 4259−4334.

(9) Mochida, M.; Kawabata, A.; Kawamura, K.; Hatsushika, H.; Yamazaki, K. Seasonal Variation and Origins of Dicarboxylic Acids in the Marine Atmosphere over the Western North Pacific. *J. Geophys. Res., D: Atmos.* **2003**, *108*, 4193.

(10) Pavuluri, C. M.; Kawamura, K.; Fu, P. Seasonal Distributions and Stable Carbon Isotope Ratios of Water-Soluble Diacids, Oxoacids, and α-Dicarbonyls in Aerosols from Sapporo: Influence of Biogenic Volatile Organic Compounds and Photochemical Aging. *ACS Earth Space Chem.* **2018**, *2*, 1220−1230.

(11) Römpp, A.; Winterhalter, R.; Moortgat, G. K. Oxodicarboxylic Acids in Atmospheric Aerosol Particles. *Atmos. Environ.* **2006**, *40*, 6846−6862.

(12) Sempéré, R.; Kawamura, K. Trans-Hemispheric Contribution of C_2 -C_{10} α, ω-Dicarboxylic Acids, and Related Polar Compounds to Water-Soluble Organic Carbon in the Western Pacific Aerosols in Relation to Photochemical Oxidation Reactions. *Global Biogeochem. Cycles* **2003**, *17*, 1069.

(13) Nozière, B.; Dziedzic, P.; Córdova, A. Inorganic Ammonium Salts and Carbonate Salts Are Efficient Catalysts for Aldol Condensation in Atmospheric Aerosols. *Phys. Chem. Chem. Phys.* **2010**, *12*, 3864−3872.

(14) Nozière, B.; Fache, F.; Maxut, A.; Fenet, B.; Baudouin, A.; Fine, L.; Ferronato, C. The Hydrolysis of Epoxides Catalyzed by Inorganic Ammonium Salts in Water: Kinetic Evidence for Hydrogen Bond Catalysis. *Phys. Chem. Chem. Phys.* **2018**, *20*, 1583−1590.

(15) Chan, M. N.; Zhang, H.; Goldstein, A. H.; Wilson, K. R. Role of Water and Phase in the Heterogeneous Oxidation of Solid and

Aqueous Succinic Acid Aerosol by Hydroxyl Radicals. *J. Phys. Chem. C* **2014**, *118*, 28978−28992.
(16) Rousová, J.; Chintapalli, M. R.; Lindahl, A.; Casey, J.; Kubátová, A. Simultaneous Determination of Trace Concentrations of Aldehydes and Carboxylic Acids in Particulate Matter. *J. Chromatogr. A* **2018**, *1544*, 49−61.
(17) Kaneko, S. On the Catalytic Decarboxylation of β-Ketoic Acid. *J. Biochem.* **1938**, *28*, 1−18.
(18) Utter, M. Metabolic Roles of Oxalacetate. *Citric Acid Cycle*; Elsevier, 1969; pp 249−296.
(19) Gelles, E. Kinetics of the Decarboxylation of Oxaloacetic Acid. *J. Chem. Soc.* **1956**, 4736−4739.
(20) Kozlowski, J.; Zuman, P. Acid-Base, Hydration-Dehydration and Keto-Enol Equilibria in Aqueous Solutions of α-Ketoacids: Study by Spectroscopy, Polarography and Linear Sweep Voltammetry. *Bioelectrochem. Bioenerg.* **1992**, *28*, 43−70.
(21) Pedersen, K. J.; Wickberg, B.; Gustafsson, C.; Sörensen, N. A. Amine Catalysis in the Decarboxylation of Oxalacetic Acid. *Acta Chem. Scand.* **1954**, *8*, 710−722.
(22) Thalji, N. K.; Crowe, W. E.; Waldrop, G. L. Kinetic Mechanism and Structural Requirements of the Amine-Catalyzed Decarboxylation of Oxaloacetic Acid. *J. Org. Chem.* **2009**, *74*, 144−152.
(23) Dawson, R. M. C.; Elliott, D.; Elliott, W. H.; Jones, K. M. *Data for Biochemical Research*; Clarendon Press: Oxford, 1959.
(24) Song, M.; Zhang, Z.; Fan, C.; Li, D.; Xu, Q.; Zhang, S. A Theoretical Study on Ethylenediamine Catalyzed Decarboxylation of Oxaloacetic Acid. *Comput. Theor. Chem.* **2013**, *1022*, 29−34.
(25) Cheng, X. Coupling and Decarboxylation Mechanism of Oxaloacetic Acid and Ethylenediamine: A Theoretical Investigation. *J. Phys. Org. Chem.* **2019**, *32*, No. e3955.
(26) Fan, C.; Song, M. Mechanistic Insights into Protonated Diamine-Catalyzed Decarboxylation of Oxaloacetate. *Lett. Org. Chem.* **2019**, *16*, 202−208.
(27) Ito, H.; Kobayashi, H.; Nomiya, K. Metal-Ion Catalyzed Decarboxylation of Oxaloacetic Acid. *J. Chem. Soc., Faraday Trans. 1* **1973**, *69*, 113−121.
(28) Pedersen, K. J.; Miquel, J. F.; Motzfeldt, K.; Finsnes, E.; Sörensen, J. S.; Sörensen, N. A. The Dissociation Constants of Pyruvic and Oxaloacetic Acid. *Acta Chem. Scand.* **1952**, *6*, 243−256.
(29) Westheimer, F. H.; Jones, W. A. The Effect of Solvent on Some Reaction Rates. *J. Am. Chem. Soc.* **1941**, *63*, 3283−3286.
(30) Epstein, S. A.; Tapavicza, E.; Furche, F.; Nizkorodov, S. A. Direct Photolysis of Carbonyl Compounds Dissolved in Cloud and Fog Droplets. *Atmos. Chem. Phys.* **2013**, *13*, 9461−9477.
(31) Arakaki, T.; Anastasio, C.; Kuroki, Y.; Nakajima, H.; Okada, K.; Kotani, Y.; Handa, D.; Azechi, S.; Kimura, T.; Tsuhako, A.; et al. A General Scavenging Rate Constant for Reaction of Hydroxyl Radical with Organic Carbon in Atmospheric Waters. *Environ. Sci. Technol.* **2013**, *47*, 8196−8203.
(32) Kaur, R.; Labins, J. R.; Helbock, S. S.; Jiang, W.; Bein, K. J.; Zhang, Q.; Anastasio, C. Photooxidants from Brown Carbon and Other Chromophores in Illuminated Particle Extracts. *Atmos. Chem. Phys.* **2019**, *19*, 6579−6594.
(33) Kaur, R.; Anastasio, C. Light Absorption and the Photoformation of Hydroxyl Radical and Singlet Oxygen in Fog Waters. *Atmos. Environ.* **2017**, *164*, 387−397.
(34) Monod, A.; Doussin, J. F. Structure-Activity Relationship for the Estimation of OH-Oxidation Rate Constants of Aliphatic Organic Compounds in the Aqueous Phase: Alkanes, Alcohols, Organic Acids and Bases. *Atmos. Environ.* **2008**, *42*, 7611−7622.
(35) Doussin, J.-F.; Monod, A. Structure-Activity Relationship for the Estimation of OH-Oxidation Rate Constants of Carbonyl Compounds in the Aqueous Phase. *Atmos. Chem. Phys.* **2013**, *13*, 11625−11641.
(36) Perdew, J. P.; Ernzerhof, M.; Burke, K. Rationale for Mixing Exact Exchange with Density Functional Approximations. *J. Chem. Phys.* **1996**, *105*, 9982−9985.
(37) Weigend, F.; Häser, M. RI-MP2: First Derivatives and Global Consistency. *Theor. Chem. Acc.* **1997**, *97*, 331−340.
(38) Weigend, F.; Häser, M.; Patzelt, H.; Ahlrichs, R. RI-MP2: Optimized Auxiliary Basis Sets and Demonstration of Efficiency. *Chem. Phys. Lett.* **1998**, *294*, 143−152.
(39) Von Arnim, M.; Ahlrichs, R. Performance of Parallel TURBOMOLE for Density Functional Calculations. *J. Comput. Chem.* **1998**, *19*, 1746−1757.
(40) Deglmann, P.; Furche, F. Efficient Characterization of Stationary Points on Potential Energy Surfaces. *J. Chem. Phys.* **2002**, *117*, 9535−9538.
(41) Klamt, A.; Schüürmann, G. COSMO: A New Approach to Dielectric Screening in Solvents with Explicit Expressions for the Screening Energy and Its Gradient. *J. Chem. Soc., Perkin Trans. 2* **1993**, 799−805.
(42) Haynes, W. M. *CRC Handbook of Chemistry and Physics*, 93rd ed.; CRC Press: Boca Raton, FL, 2012.
(43) Schäfer, A.; Klamt, A.; Sattel, D.; Lohrenz, J. C. W.; Eckert, F. COSMO Implementation in TURBOMOLE: Extension of an Efficient Quantum Chemical Code towards Liquid Systems. *Phys. Chem. Chem. Phys.* **2000**, *2*, 2187−2193.
(44) Balasubramani, S. G.; Chen, G. P.; Coriani, S.; Diedenhofen, M.; Frank, M. S.; Franzke, Y. J.; Furche, F.; Grotjahn, R.; Harding, M. E.; Hättig, C.; et al. TURBOMOLE: Modular Program Suite for Ab Initio Quantum-Chemical and Condensed-Matter Simulations. *J. Chem. Phys.* **2020**, *152*, 184107.
(45) Mekic, M.; Brigante, M.; Vione, D.; Gligorovski, S. Exploring the Ionic Strength Effects on the Photochemical Degradation of Pyruvic Acid in Atmospheric Deliquescent Aerosol Particles. *Atmos. Environ.* **2018**, *185*, 237−242.
(46) Zhou, W.; Mekic, M.; Liu, J.; Loisel, G.; Jin, B.; Vione, D.; Gligorovski, S. Ionic Strength Effects on the Photochemical Degradation of Acetosyringone in Atmospheric Deliquescent Aerosol Particles. *Atmos. Environ.* **2019**, *198*, 83−88.
(47) Herrmann, H. Kinetics of Aqueous Phase Reactions Relevant for Atmospheric Chemistry. *Chem. Rev.* **2003**, *103*, 4691−4716.
(48) Ervens, B.; Turpin, B. J.; Weber, R. J. Secondary Organic Aerosol Formation in Cloud Droplets and Aqueous Particles (AqSOA): A Review of Laboratory, Field and Model Studies. *Atmos. Chem. Phys.* **2011**, *11*, 11069−11102.
(49) Huang, C.-L.; Wu, C.-C.; Lien, M.-H. Ab Initio Studies of Decarboxylations of the β-Keto Carboxylic Acids $XCOCH_2COOH$ (X = H, OH, and CH_3). *J. Phys. Chem. A* **1997**, *101*, 7867−7873.
(50) Staikova, M.; Oh, M.; Donaldson, D. J. Overtone-Induced Decarboxylation: A Potential Sink for Atmospheric Diacids. *J. Phys. Chem. A* **2005**, *109*, 597−602.
(51) Seeman, J. I. The Curtin-Hammett Principle and the Winstein-Holness Equation: New Definition and Recent Extensions to Classical Concepts. *J. Chem. Educ.* **1986**, *63*, 42−48.
(52) Luo, M.; Shemesh, D.; Sullivan, M. N.; Alves, M. R.; Song, M.; Gerber, R. B.; Grassian, V. H. Impact of PH and NaCl and $CaCl_2$ Salts on the Speciation and Photochemistry of Pyruvic Acid in the Aqueous Phase. *J. Phys. Chem. A* **2020**, *124*, 5071−5080.
(53) Ray, D.; Ghosh, S. K.; Raha, S. Impacts of Some Co-Dissolved Inorganics on in-Cloud Photochemistry of Aqueous Brown Carbon. *Atmos. Environ.* **2020**, *223*, 117250.
(54) Leussing, D. L.; Raghavan, N. V. Ethylenediamine and Aminoacetonitrile Catalyzed Decarboxylation of Oxalacetate. *J. Am. Chem. Soc.* **1980**, *102*, 5635−5643.
(55) Smith, J. N.; Barsanti, K. C.; Friedli, H. R.; Ehn, M.; Kulmala, M.; Collins, D. R.; Scheckman, J. H.; Williams, B. J.; McMurry, P. H. Observations of Aminium Salts in Atmospheric Nanoparticles and Possible Climatic Implications. *Proc. Natl. Acad. Sci. U.S.A.* **2010**, *107*, 6634−6639.
(56) Surratt, J. D.; Kroll, J. H.; Kleindienst, T. E.; Edney, E. O.; Claeys, M.; Sorooshian, A.; Ng, N. L.; Offenberg, J. H.; Lewandowski, M.; Jaoui, M.; et al. Evidence for Organosulfates in Secondary Organic Aerosol. *Environ. Sci. Technol.* **2007**, *41*, 517−527.
(57) Minerath, E. C.; Elrod, M. J. Assessing the Potential for Diol and Hydroxy Sulfate Ester Formation from the Reaction of Epoxides in Tropospheric Aerosols. *Environ. Sci. Technol.* **2009**, *43*, 1386−1392.

https://doi.org/10.1021/acsearthspacechem.1c00025
ACS Earth Space Chem. 2021, 5, 931−940

(58) Surratt, J. D.; Chan, A. W. H.; Eddingsaas, N. C.; Chan, M.; Loza, C. L.; Kwan, A. J.; Hersey, S. P.; Flagan, R. C.; Wennberg, P. O.; Seinfeld, J. H. Reactive Intermediates Revealed in Secondary Organic Aerosol Formation from Isoprene. *Proc. Natl. Acad. Sci. U.S.A.* **2010**, *107*, 6640−6645.
(59) Nozière, B.; Dziedzic, P.; Córdova, A. Products and Kinetics of the Liquid-Phase Reaction of Glyoxal Catalyzed by Ammonium Ions (NH_4^+). *J. Phys. Chem. A* **2009**, *113*, 231−237.
(60) Hay, R.; Bond, M. Kinetics of the Decarboxylation of Acetoacetic Acid. *Aust. J. Chem.* **1967**, *20*, 1823−1828.
(61) Pedersen, K. J. The Ketonic Decomposition of Beta-Keto Carboxylic Acids. *J. Am. Chem. Soc.* **1929**, *51*, 2098−2107.

https://doi.org/10.1021/acsearthspacechem.1c00025
ACS Earth Space Chem. 2021, 5, 931−940